Search for Exotic Phenomena using Events with Same Charge Dileptons + b-Jets at 13 TeV with ATLAS

Sarah L. Jones, on behalf of the ATLAS Collaboration

Department of Physics, 1118 E 4th St, University of Arizona, Tucson, AZ 85721

A search is presented using events with b-jets, sizable missing transverse energy and total transverse momentum from leptons and jets (H_T), and at least two leptons with the same charge in the final state (three lepton final states are also considered). The Standard Model (SM) processes that produce final states of this sort are relatively rare, so the SM backgrounds for this search are low. Several signal models are explored, which could produce an enhanced production rate for final states with same charge dileptons. The signal models explored here are Vector-like Quarks B, T, and $T_{5/3}$, and several 4-top ($t\bar{t}t\bar{t}$) signatures: Standard Model production, contact interaction, and a model with two Universal Extra Dimensions under the real projective plane geometry (2UED/RPP).

1 Introduction

Several theoretical models predict new particles that may provide an answer to the nature of dark matter or a mechanism for naturally stabilizing the Standard Model (SM) Higgs mass at the observed value of 125 GeV.[1,2] This search looks for evidence of different beyond the Standard Model (BSM) signal models that produce particles that decay to two leptons[a] of the same charge plus associated missing transverse energy and b-jets. Among the models presented here are those that include Vector-Like Quarks (VLQ) of the varieties T, B, and $T_{5/3}$, and models that predict enhanced 4-top ($t\bar{t}t\bar{t}$) production from SM, contact interaction (CI), or via two universal extra dimensions under the real projective plane geometry (2UED/RPP). Figure 1 shows leading order Feynman diagrams for $T_{5/3}$ pair production and the contact interaction model for 4-top production.

The VLQ production modes this analysis is sensitive to are pair and single production of $T_{5/3}$ and pair production of T and B, because these have a likely chance of producing two same charge leptons or multiple leptons. The decay modes of interest include $T_{5/3} \rightarrow Wt$ and for the T and B VLQ varieties, charged current, $T \rightarrow Wb$ and $B \rightarrow Wt$, and neutral current $T \rightarrow Zt/Ht$ and $B \rightarrow (Zb/Hb)$. The VLQ are assumed to couple only to 3rd generation quarks in this search.

Previous searches for VLQ and 4-top production at ATLAS and CMS with $\sqrt{s} = 8$ TeV data did not reveal evidence of a significant excess of same charge dilepton production. However, the ATLAS search[3] did show a modest excess of about 2.5σ in the signal regions with the highest transverse energy, missing transverse energy, and higher number of b-jets. This excess was investigated with the early Run II collision data, totaling 3.2 fb^{-1} at $\sqrt{s} = 13$ TeV.[4] The results with this dataset are presented in this conference. An analysis with the full $\sqrt{s} = 13$ TeV dataset is currently being done, where the signal regions are optimized to better account for the increase in energy.

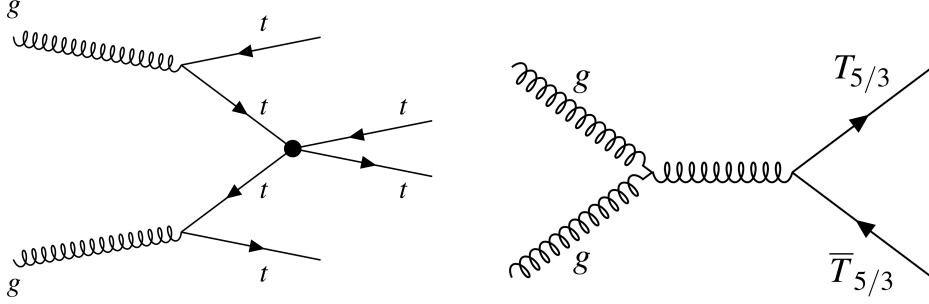[a]In this context, when referring to leptons, only muons and electrons are considered.

Figure 1 – Tree-level diagrams for two signals searched for in this analysis. On the left, the contact interaction model for 4-top production is shown. On the right, pair production via gluon-gluon fusion is shown for $T_{5/3}$ vector-like quarks. Note this mode of pair production for $T_{5/3}$ is also applicable to the T and B vector-like quarks searched for in this analysis.

2   Background Estimation

There are two major background categories in this analysis. The first encompasses all the irreducible backgrounds from SM processes that produce real same-sign dilepton pairs plus associated jets in the final state. Such processes are well-understood and all sources must be taken into account. The contributions come from $t\bar{t}+V$, where $V = W$, Z, and to a lesser extent H, diboson and triboson processes, and three top quark processes. Irreducible backgrounds are modeled with MC and normalized to the appropriate luminosity to compare with the data.

The second major category of backgrounds is referred to as the data-driven background because modeling of the backgrounds in this category is done with data instead of MC. This is because it is difficult to accurately simulate these backgrounds. There are two backgrounds contributing to the data-driven background estimation in this analysis: (1) charge mis-identified electrons and (2) fake and non-prompt leptons.

Charge mis-identified electrons are electrons that have had their charge mis-measured leading to a mis-identified pair of same-sign dileptons, when in fact the pair is opposite-sign. This background is negligible for muons since the ATLAS muon system has a long lever-arm, muons are unlikely to radiate photons at the energies muons are typically produced in ATLAS, and the charge of a muon is measured in both the inner detector as well as the Muon Spectrometer. Calculating the rate, ε, at which the charge of an electron is mis-measured is done using $Z \to ee$ data events in the Z-peak region ($|m_{ee} - m_Z| < 10$ GeV). The rates are binned in electron p_T and η and extracted by maximizing the Poisson likelihood for a same-sign electron pair in each bin. An overall weight is applied to opposite-sign events to estimate the total same-sign events where one electron has its charge mis-measured.

The fake and non-prompt lepton background is estimated by first defining a sample consisting of single lepton events with the isolation requirements on the lepton relaxed, creating a *loose* set of leptons. A *tight* sample of leptons, required to be a strict subset of the *loose* sample, is defined by using the same definition of leptons as is used in the main analysis, including an isolation requirement. Then, efficiencies for a lepton to pass the *tight* criteria (isolation) are measured in control regions enriched in either real leptons or fake leptons. Real and fake efficiencies are extracted from the corresponding control region and binned in lepton p_T, η, and $\Delta R(\ell, \text{closest jet})$. Event characteristics, such as the trigger used to fire the event and the number of b-tagged jets in the event, are also accounted for in the efficiencies since different event characteristics can influence the real and fake efficiencies in different ways.

Once the efficiencies are measured for electrons and muons, a Poisson likelihood approach is used to estimate the overall number of fake leptons in the control and signal regions for this analysis. The Poisson likelihood is based on the familiar Matrix Method, where the total number of tight fake leptons depends on the real and fake efficiencies measured in control samples and the

total number of loose and tight leptons in a sample. The Poisson likelihood approach uses the same Matrix Method but applies a bin-by-bin likelihood fit on a sample, instead of calculating an event-by-event weight which the Matrix Method normally employs. This approach was shown to provide more stability for the estimation of the fakes background.

The background estimation is validated in a set of control and validation regions where the full data-driven estimation and total MC backgrounds are compared with data. Once the backgrounds are validated, the data is unblinded in the signal regions. The analysis strategy is a simple 'cut-and-count' method, where for each signal region the total predicted background events and data yields are compared.

3 Systematic Uncertainties

Systematic uncertainties primarily come from uncertainties on the cross section and luminosity, as well as from simulation systematics. Uncertainties from the jet energy scale and resolution, lepton identification efficiency, and b-tagging efficiency also contribute to the overall background uncertainty. The fake and non-prompt lepton background contributes a large portion of the total systematic uncertainties in the signal regions, about 54%. The charge mis-id background contributes about 25% of the total background uncertainties in the signal regions. Both data-driven background systematics are derived from variations in the calculation of the efficiencies or rates used to estimate the backgrounds.

4 Results

Similar signal regions are defined for the 4-top and vector-like quark signal models since they share a similar final state topology. However, the distributions for these signals in some kinematic variables differs somewhat. Therefore, eight orthogonal signal regions are defined to optimize certain regions' signal significance providing greater sensitivity to the signal models. The channels, $e^{\pm}e^{\pm}$, $\mu^{\pm}\mu^{\pm}$, $e^{\pm}\mu^{\pm}$, eee, $e\mu\mu$, $ee\mu$, $\mu\mu\mu$, are combined and further categorized by kinematic cuts on $E_{\mathrm{T}}^{\mathrm{miss}}$, H_{T}, the number of b-jets and other jets into the eight regions. These cuts are summarized in Table 1 defining the signal regions.

Table 1: Signal region definitions.

Definition			Region Name
$N_j \geq 2$ and $e^{\pm}e^{\pm}$, $\mu^{\pm}\mu^{\pm}$, $e^{\pm}\mu^{\pm}$, eee, $e\mu\mu$, $ee\mu$, $\mu\mu\mu$			
$400 < H_{\mathrm{T}} < 700$ GeV	$N_b = 1$	$E_{\mathrm{T}}^{\mathrm{miss}} > 40$ GeV	SR0
	$N_b = 2$		SR1
	$N_b \geq 3$		SR2
$H_{\mathrm{T}} \geq 700$ GeV	$N_b = 1$	$40 < E_{\mathrm{T}}^{\mathrm{miss}} < 100$ GeV	SR3
		$E_{\mathrm{T}}^{\mathrm{miss}} \geq 100$ GeV	SR4
	$N_b = 2$	$40 < E_{\mathrm{T}}^{\mathrm{miss}} < 100$ GeV	SR5
		$E_{\mathrm{T}}^{\mathrm{miss}} \geq 100$ GeV	SR6
	$N_b \geq 3$	$E_{\mathrm{T}}^{\mathrm{miss}} > 40$ GeV	SR7

The expected total backgrounds are compared with the data yields in the signal regions as shown in Figure 2. The total statistical and systematic uncertainties are included for each region. The $\mathrm{CL_s}$ method[5] is used to assess the consistency between the observed yields in each region with each signal model. Since no observed excess of data events is found, upper limits on the cross section and lower limits on the mass are set, at the 95% CL, on the various VLQ models. Limits on the 4-top models are also set. The lower limit on the contact interaction coupling constant and the pair production $T_{5/3}$ limits are shown in Figure 3.
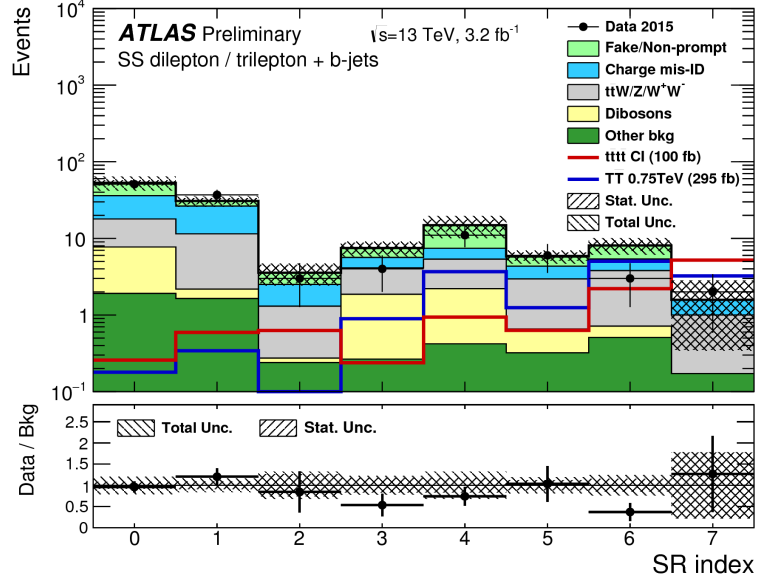
Figure 2 – Summary plot of total background and data in the eight signal regions defined in Table 1. Two signal models are also overlaid to show the relative sensitivity each signal region has for the particular model.
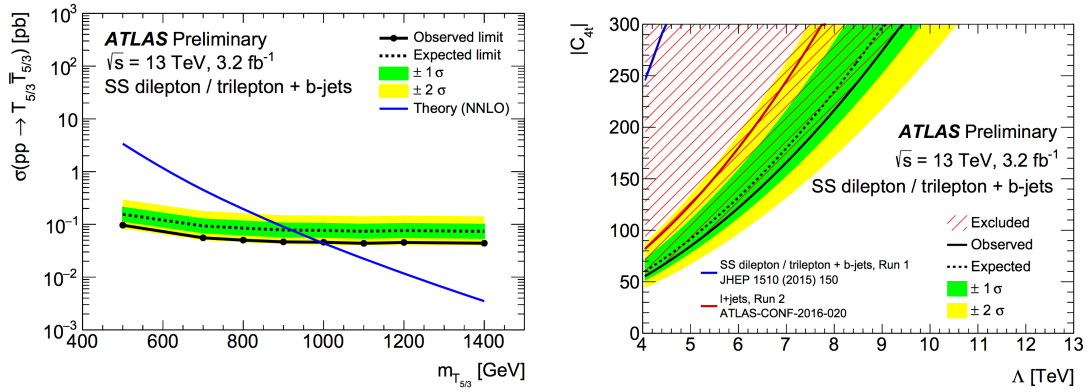

Figure 3 – Limits at the 95% CL for the pair production of $T_{5/3}$ (left) and contact interaction for the 4-top signal model (right). The yellow and green colored bands represent the $\pm 1\sigma$ and $\pm 2\sigma$ standard deviations for the expected limit. The solid curve shows the observed limits.

Acknowledgements

References

1. ATLAS Collaboration Phys. Lett. B **716**, 1 (2012).
2. CMS Collaboration Phys. Lett. B **716**, 30 (2012).
3. ATLAS Collaboration JHEP **03**, 041 (2015).
4. ATLAS Collaboration **ATLAS-CONF-2016-032** Jun 2016.
5. A.L. Read J. Phys. G **28**, 2693 (2002).